

This mechanism is schematically visualized in Figure 8. After the Pt-N1 bond, which is weakened by the N7-protonation, is broken, a rapid protonation (N1) and deprotonation (N7) can take place (see Figure 8b). Meanwhile, the platinum moiety can move around from the N1 to the N7 and bind to this site, meanwhile remaining attached to the eGua by hydrogen bonding to the O6. This N1 to N7 migration will occur very rapidly, since no inactivation of the hydrogen-bonded Pt moiety by means of substitution of the coordinated water by Cl⁻ or NH₃ is observed. Additional support for this mechanism was obtained by the observation that the isomerization yielded more metal-free eGua when performed at pH 1.5 (data not shown). In that case, a larger amount of the intermediate compound is protonated at both the N1 and the N7, making the ultimate formation of the N7 adduct less probable.

Another migration model, assuming two head-to-tail stacked N1 adducts in which the two platinum moieties jump at the same time from the N1 to the N7 of the stacking eGua is not very likely. Stacking interactions are very sensitive to ionic strength differences, and in our case the addition of 0.1 M salt did not induce any difference in the migration rate (*vide supra*).

It has been reported that a platinum migration mechanism might also occur for inosine.¹⁶ In that case, however, an N7 to N1 isomerization at pH 5-6 was described, with a dinuclear N1,N7 species as intermediate. These results are, however, not applicable to our study, as in our case an opposite migration from

N1 to N7 occurs and the dinuclear compound [Pt(dien)]₂(μ-eGua-N1,N7) appears to be very stable at pH 2.8. The difference therefore must originate from the amine group, which is not present at C2 in inosine.

Concluding Remarks. In this study, the synthesis and characterization of various platinum products with 9-ethylguanine have been presented. An interesting migration of the platinum moiety from N1 to N7—which probably occurs intramolecularly—could be studied in detail. Since platinum adducts with nucleobase are generally looked upon as very stable, this finding of instable mononuclear eGua-N1 adducts is of great importance and can be of relevance for future studies of metal-DNA interactions.

Acknowledgment. This study was supported in part by the Netherlands Foundation of Chemical research (SON) with financial aid from the Netherlands Organization for the Advancement of Pure Research (ZWO), through Grant 11-28-17. Stimulating discussions with the group of Prof. Dr. J. C. Chottard (Paris), made possible through the sponsorship of the French-Dutch cultural agreement, are gratefully acknowledged. Prof. Dr. L. G. Marzilli (Emory University, Atlanta, GA), F. J. Dijt, C. J. van Garderen, and H. P. J. M. Noteborn are thanked for the critical reading of the manuscript. We are indebted to the Netherlands Organization for the Fight against Cancer for their financial support and to Johnson Matthey Chemicals, Ltd. (Reading, England), for their generous loan of K₂PtCl₄.

Contribution from the Institut für Anorganische Chemie, Technische Hochschule Darmstadt, D-6100 Darmstadt, West Germany, and Department of Chemistry, Western Washington University, Bellingham, Washington 98225

Metal Complexes of Tetrapyrrole Ligands. 43.¹ Nickel(II) 5,15-Dialkyl-5,15-dihydro-2,3,7,8,12,13,17,18-octaethylporphyrins (Decaalkylporphodimethenes): Isolation of a New Stereoisomer and ¹H NMR Spectroscopy

Andreas Botulinski,^{2a} Johann W. Buchler,^{*2a} and Mark Wicholas^{*2b}

Received September 2, 1986

The synthesis and spectral characterization of novel nickel(II) 5,15-dialkyl-5,15-dihydro-2,3,7,8,12,13,17,18-octaethylporphyrins, Ni(OEPR₂) (*aa-1-aa-4*), are described wherein the bulky 5,15-substituents (R = Me, Et, *i*-Pr, and *t*-Bu) assume the syn-axial conformation. The isolation of a hitherto unknown anti (axial-equatorial) isomer of the diisopropyl derivative Ni(OEPPR₂) (*ae-3*) is reported, and its configuration is deduced from a detailed analysis of the NMR spectra of all the nickel chelates. The chemical shifts are influenced by ring current effects of the individual pyrrole units, the folding of the tetrapyrrole system, the saddlelike deformation of the pyrromethene halves, and long-range shielding by neighboring groups.

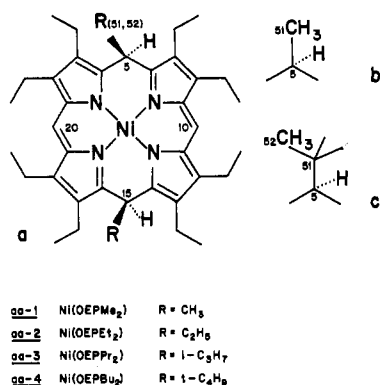
The occurrence of reduced heme proteins in natural systems has generated much recent interest in the chemistry of simple chlorins (2,3-dihydroporphyrins) and isobacteriochlorins (2,3,7,8-tetrahydroporphyrins).³⁻⁵ Both are species in which

hydrogenation of the porphyrin ring has occurred at peripheral double bonds without effect upon the macrocyclic conjugation. A different class of hydrogenated porphyrins are the less commonly encountered 5,15-dialkyl-5,15-dihydroporphyrins (decaalkylporphodimethenes). Here, hydrogenation has occurred at two opposite meso positions and the ring conjugation is destroyed. Porphodimethenes readily coordinate to metal ions via the four pyrrole nitrogens, and we reported most recently the synthesis and ¹H NMR spectra of a series of paramagnetic cobalt(II) porphodimethenes.⁶ The complexes specifically discussed herein are the nickel(II) 5,15-dialkyl-2,3,7,8,12,13,17,18-octaethylporphodimethenes, Ni(OEPR₂) (see Figure 1), which are best prepared from zinc(II) octaethylporphyrin, Zn(OEP), by reduction with sodium anthracenide followed by alkylation with alkyl halide,

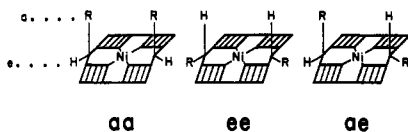
- (1) Part 42: Buchler, J. W.; Elsässer, K.; Kihn-Botulinski, M.; Scharbert, B.; Tansil, S. *ACS Symp. Ser.* **1986**, No. 321, 94.
- (2) (a) Technische Hochschule Darmstadt. (b) Western Washington University.
- (3) (a) Strauss, S. H.; Holm, R. H. *Inorg. Chem.* **1982**, *21*, 863. (b) Strauss, S. H.; Silber, M. E.; Ibers, J. A. *J. Am. Chem. Soc.* **1983**, *105*, 4108. (c) Suh, M. P.; Swepston, P. N.; Ibers, J. A. *J. Am. Chem. Soc.* **1984**, *106*, 5164. (d) Galluci, J.; Swepston, P. N.; Ibers, J. A. *Acta Crystallogr., Sect. B: Struct. Crystallogr. Cryst. Chem.* **1982**, *B38*, 2134.
- (4) Kratky, C.; Waditschka, R.; Angst, X.; Johansen, J. E.; Plaquevent, J. C.; Schreiber, J.; Eschenmoser, A. *Helv. Chim. Acta* **1985**, *68*, 1312.
- (5) (a) Barkigia, K. M.; Jajer, J.; Chang, C. K.; Young, R. *J. Am. Chem. Soc.* **1984**, *106*, 6457. (b) Smith, K. M.; Goff, D. A. *J. Am. Chem. Soc.* **1985**, *107*, 4954.

- (6) Botulinski, A.; Buchler, J. W.; Tonn, B.; Wicholas, M. *Inorg. Chem.* **1985**, *24*, 3239.

demetalation, and insertion of nickel(II).⁷ The isomer commonly isolated is that in which the R groups are syn-axial; i.e., upon alkylation of the porphyrin dianion, the alkyl groups preferentially come in from the same side. This syn-axial, or "aa", configuration is depicted schematically as

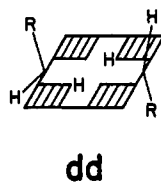


The crystal structure of Ni(OEPMe₂), the dimethyl derivative aa-1, has been previously described.⁸ The macrocycle is decidedly nonplanar with significant folding about the 5,15-axis and ruffling of the pyrrole rings. This clearly is a consequence of the saturation at C5,15 and is common to all metal porphodimethenes whose structures have been determined.⁹ The small Ni²⁺ ion in the center of the porphodimethene necessitates the rooflike folding of the macrocycle,⁸ and three stereoisomers are possible on the basis of the disposition of the R groups. These are the syn-axial ("aa"), anti-axial-equatorial ("ae"), and syn-equatorial ("ee") isomers:



The order of stability of these stereoisomers, either free ligand or metal complex, should be aa > ae > ee on the basis of steric factors. This becomes obvious upon inspection of space-filling molecular models. When the alkyl groups, R, are equatorial, steric crowding by the four adjacent peripheral ethyl groups sitting at the "gable" parts of the "rooflike" folded porphodimethene occurs; thus the axial orientation of R is preferred.

The stereochemistry of the metal-free porphodimethenes is somewhat more complex. During the synthesis of aa-H₂(OEPR₂), small quantities of a second diastereoisomer were isolated after careful column chromatography on alumina.¹⁰ At first tentatively assigned the ee configuration, this isomer was subsequently shown by X-ray crystallography of H₂(OEPPR₂) to have the planar anti configuration¹¹ (dd) with an inversion center:



- (7) Buchler, J. W.; Puppe, L. *Justus Liebig's Ann. Chem.* **1970**, *740*, 142.
- (8) Dwyer, P. N.; Buchler, J. W.; Scheidt, W. R. *J. Am. Chem. Soc.* **1974**, *96*, 2789.
- (9) (a) Buchler, J. W.; Lay, K. L.; Young, J. L.; Scheidt, W. R. *Angew. Chem., Int. Ed. Engl.* **1982**, *21*, 432. (b) Buchler, J. W.; Dreher, C.; Lay, K. L.; Young, J. L.; Scheidt, W. R. *Inorg. Chem.* **1983**, *22*, 888. (c) Buchler, J. W.; Lay, K. L.; Smith, P. D.; Scheidt, W. R.; Rupprecht, G. A.; Kenny, J. E. *J. Organomet. Chem.* **1976**, *110*, 109. (d) Dwyer, P. L.; Puppe, L.; Buchler, J. W.; Scheidt, W. R. *Inorg. Chem.* **1975**, *14*, 1982.
- (10) Botulinski, A.; Buchler, J. W.; Lay, K. L.; Stoppa, H. *Liebigs Ann. Chem.* **1984**, 1259.
- (11) Botulinski, A.; Buchler, J. W.; Lay, K. L.; Abbes, N. E.; Scheidt, W. R., to be submitted for publication in *Liebigs Ann. Chem.*

However, in CDCl₃ solution the ¹H NMR spectra indicated that the planar dd isomer had partially converted to the folded ae form of H₂(OEPR₂), and both were present in a 4:1 ratio, respectively.

Metalloporphodimethenes containing the macrocycle in an anti configuration, either dd or ae, have never been reported previously. This paper describes the preparation and ¹H NMR spectra of the syn-axial nickel(II) porphodimethenes, aa-1-aa-4, and the first anti metalloporphodimethene, Ni(OEPPR₂) (ae-3), which is prepared by reaction of nickel(II) acetate and dd-H₂(OEPR₂) in glacial acetic acid. All configurations can be deduced from the ¹H NMR spectra, which are very sensitive to slight changes in conformation of the porphodimethene skeleton that occur when the steric requirements of the alkyl groups are increased.

Experimental Section

Materials and Methods. The metal-free decaalkylporphodimethenes aa-H₂(OEPR₂) (R = Me, Et, *i*-Pr, and *t*-Bu) as well as dd-H₂(OEPR₂) are prepared as described in the literature,¹⁰ where the aa isomers are termed "normal" and the dd isomers "anomalous". Microanalyses were performed by F. Roth, Institut für Organische Chemie und Biochemie, Technische Hochschule Darmstadt. UV/vis, IR, NMR, and mass spectra were run respectively with the following instruments: Unicam SP 800 (in toluene); Perkin-Elmer 397 (KBr pellets); Bruker WM 300 (20 °C, CDCl₃, internal Me₄Si), Varian MAT 311 A (data system SS 100 MS, direct-insertion probe, electron impact ionization, source temperature 250 °C, mass numbers *A* and (in parentheses) relative intensities and assignments are noted). Computer simulations of NMR spectra were done with the program PANIC, which is part of the Bruker software package.

Synthesis of Nickel(II) Decaalkylporphodimethenes, Ni(OEPR₂) (aa-1-aa-4 and ae-3). Syn-axial species, aa-1-aa-4, are prepared from the corresponding H₂(OEPR₂) (R = Me, Et, *i*-Pr, and *t*-Bu) according to the described procedures for aa-1⁷ from nickel(II) acetate by boiling 1 h in glacial acetic acid and sodium acetate under argon, chromatography on alumina (Grade IV, n; in cyclohexane), and crystallization from cyclohexane.

syn-axial-(5,15-Diethyl-5,15-dihydro-2,3,7,8,12,13,17,18-octaethylporphyrinato)nickel(II), Ni(OEPEt₂) (aa-2): from 101 mg (0.17 mmol) of aa-H₂(OEPEt₂), 0.5 g (2.0 mmol) of Ni(OAc)₂, and 1.0 g of NaOAc in 70 mL of HOAc; yield 78 mg (70%); mp 268 °C dec. Anal. Calcd for aa-2, C₄₀H₅₄N₄Ni (mol wt 649.6): C 73.95; H, 8.38; N, 8.62. Found: C, 73.07; H, 8.27; N, 8.54. UV/vis (λ_{max} (log ε)): 440 (4.74), 548 nm (4.29). IR: 1615, 1213, 1007, 875 cm⁻¹ (porphodimethene bands^{6,10,11}). Mass spectrum (*A*): 648 (38%, M⁺), 619 (100%, M⁺ - Et), 590 (96%, M⁺ - 2 Et), 324 (9%, M²⁺), 309 (13%, M²⁺ - Et), 295 (44%, M²⁺ - 2 Et).

syn-axial-(5,15-Diisopropyl-5,15-dihydro-2,3,7,8,12,13,17,18-octaethylporphyrinato)nickel(II), Ni(OEPPr₂) (aa-3): from 35 mg (0.05 mmol) of aa-H₂(OEPPr₂), 150 mg (0.6 mmol) of Ni(OAc)₂, and 350 mg (2.5 mmol) of NaOAc in 70 mL of HOAc; yield 20 mg (52%); mp 280 °C dec. Anal. Calcd for aa-3, C₄₂H₅₈N₄Ni (mol wt 677.7): C, 74.74; H, 8.62; N, 8.26. Found: C, 74.27; H, 8.76; N, 8.27. UV/vis (λ_{max} (log ε)): 442 (4.75), 550 nm (4.26). IR: 1615, 1213, 1008, 901 cm⁻¹ (see aa-2). Mass spectrum (*A*): 676 (17%, M⁺), 633 (38%, M⁺ - Pr), 604 (15%, M⁺ - Pr - Et), 590 (100%, M⁺ - 2 Pr), 338 (1%, M²⁺), 317 (1%, M²⁺ - Pr), 295 (3%, M²⁺ - 2 Pr).

syn-axial-(5,15-Di-*tert*-butyl-5,15-dihydro-2,3,7,8,12,13,17,18-octaethylporphyrinato)nickel(II), Ni(OEPBu₂) (aa-4): from 101 mg (0.15 mmol) of aa-H₂(OEPBu₂), 0.5 g (2.0 mmol) of Ni(OAc)₂, and 1.0 g (7.3 mmol) of NaOAc in 70 mL of HOAc; yield 77 mg (70%); mp 278 °C dec. Anal. Calcd for aa-4, C₄₄H₆₆N₄Ni (mol wt 705.7): C, 74.88; H, 8.85; N, 7.94. Found: C, 74.26; H, 8.92; N 7.88. UV/vis (λ_{max} (log ε)): 442 (4.78), 514 (4.22, shoulder), 550 nm (4.31). IR: 1626, 1230, 1010, 874 cm⁻¹ (see aa-2). Mass spectrum (*A*): 704 (3%, M⁺), 647 (10%, M⁺ - Bu), 618 (1%, M⁺ - Bu - Et), 591 (100%, M⁺ - 2 Bu), 296 (1%, M²⁺ - 2 Bu).

anti-axial-equatorial-(5,15-Diisopropyl-5,15-dihydro-2,3,7,8,12,13,17,18-octaethylporphyrinato)nickel(II), Ni(OEPPr₂) (ae-3). An 11-mg (0.02-mmol) amount of dd-H₂(OEPPr₂), 50 mg (0.2 mmol) of Ni(OAc)₂, and 100 mg (0.07 mmol) of NaOAc are heated to boiling in 70 mL HOAc that was previously deoxygenated under argon. After it is cooled, the reaction mixture is taken to dryness, and the residue is extracted with CH₂Cl₂ and filtered. The CH₂Cl₂ solution is shaken with dilute aqueous ammonia and again taken to dryness. The resulting solid is dissolved in cyclohexane and chromatographed on alumina (grade IV, n; 20 × 3 cm) under N₂. The first half of the greenish red band yields pure aa-Ni(OEPPr₂) (aa-3). The second half of the band is collected separately and evaporated to dryness. The residue is then recrystallized twice from pyridine. The resulting crystals contain both aa-3 and ae-

Table I. ¹H NMR Spectra^a of the Nickel Porphodimethenes Ni(OEPR₂) and Nickel Octaethylporphyrin, Ni(OEP)

compd	H10,20	H5,15	α-CH ₂	β-CH ₃	R (H51,52)
<i>aa-1</i>	6.67 (s, 2 H)	3.97 (q, 2 H, <i>J</i> = 7.0)	2.48 (m, 8 H) 2.38 (q, 8 H)	1.12 (t, 12 H, <i>J</i> = 7.6) 1.05 (t, 12 H, <i>J</i> = 7.6)	2.22 (d, 6 H, <i>J</i> = 7.0)
<i>aa-2</i>	6.65 (s, 2 H)	3.76 (t, 4 H, <i>J</i> = 7.0)	2.48 (m, 8 H) 2.33 (q, 8 H)	1.20 (t, 12 H, <i>J</i> = 7.6) 1.04 (t, 12 H, <i>J</i> = 7.6)	2.79 (m, 4 H) 1.18 (t, 12 H, <i>J</i> = 7.4) 3.51 (m, 2 H)
<i>aa-3</i>	6.58 (s, 2 H)	3.56 (d, 2 H, <i>J</i> = 6.3)	2.47 (m, 8 H) 2.33 (q, 8 H)	1.13 (t, 12 H, <i>J</i> = 7.6) 1.03 (t, 12 H, <i>J</i> = 7.6)	1.26 (d, 12 H, <i>J</i> = 6.3)
<i>ae-3</i>	6.41 (s, 2 H)	5.43 (d, 2 H, <i>J</i> = 12.8) ^b 3.36 (d, 2 H, <i>J</i> = 9.6) ^c	2.38 (m, 4 H) 2.47 (m, 4 H) 2.33 (m, 4 H)	1.06 (t, 6 H, <i>J</i> = 7.6) 1.10 (t, 6 H, <i>J</i> = 7.6) 1.03 (t, 6 H, <i>J</i> = 7.6)	2.63 (m, 1 H) ^c 4.01 (m, 1 H) ^b 1.27 (d, 6 H, <i>J</i> = 6.6) ^b
<i>aa-4</i>	6.50 (s, 2 H)	3.87 (s, 2 H)	2.24 (m, 4 H) 2.48 (m, 8 H) 2.38 (m, 8 H)	1.00 (t, 6 H, <i>J</i> = 7.6) 1.13 (t, 12 H, <i>J</i> = 7.6) 1.02 (t, 12 H, <i>J</i> = 7.6)	1.17 (d, 6 H, <i>J</i> = 6.1) ^c 1.55 (s, 18 H)
Ni(OEP)	9.80		3.94	1.80	

^aAll spectra were run at 300 MHz and 20 °C in CDCl₃. δ values are relative to Me₄Si; units of *J* are Hz. ^bH axial. ^cH equatorial.

Ni(OEPR₂) (*ae-3*). With the use of a microscope, the violet needles of *aa-3* (total yield after combination with the first crop: 2.5 mg, 21%) were separated from the brown cubes of *ae-3* (2.0 mg, 17%); mp 225 °C dec. Mol wt: calcd for C₄₀H₅₄N₄Ni, 676.40; found by mass spectrometry 676.40. Mass spectrum (*A*): 676 (16%, M⁺), 633 (64%, M⁺ - Pr), 604 (2%, M⁺ - Pr - Et), 590 (100%, M⁺ - 2 Pr), 338 (5%, M²⁺), 317 (3%, M²⁺ - Pr), 295 (11%, M²⁺ - 2 Pr). UV/vis (λ_{max} (log ε)): 444 (4.75), 568 nm (4.15). IR: 1608, 1214, 1009, 960 cm⁻¹ (see *aa-2*).

Results and Discussion

Insertion of nickel(II) into the porphodimethene macrocycle occurs readily for both the syn-axial and anti stereoisomers of H₂(OEPR₂) when nickel(II) acetate is used in buffered glacial acetic acid. From *syn-axial*-H₂(OEPR₂), the nickel(II) chelates Ni(OEPR₂), where R = Et, *i*-Pr, and *t*-Bu, were isolated following a procedure described previously for Ni(OEPMe₂).⁷ In all cases, the syn-axial configuration was retained. The nickel(II) insertion reaction with *anti*-H₂(OEPR₂), however, requires special comment. As the anti isomers of H₂(OEPR₂) are formed in minor amounts during the reductive alkylation, nickel insertion was attempted only for *anti*-H₂(OEPR₂), which exists in the solid state as the dd stereoisomer. For this reaction and subsequent chromatography, oxygen must be excluded, otherwise dehydrogenation of the porphodimethene at C5,15 will occur.⁷ Nevertheless, a quantitative conversion of *anti*-H₂(OEPR₂) into its nickel chelate is not observed. Instead, at best a 1:1 mixture of *aa-3* and *ae-3* is obtained.¹² Thus, during metal insertion, isomerization of the anti species to the syn-axial species occurs. It has been shown independently that the anti → syn isomerization can be effected quantitatively by heating *anti*-H₂(OEPR₂) for 1 h in glacial acetic acid in the absence of metal ions.¹⁰ Such an isomerization necessitates either bond breaking at the C5,15 carbon or dehydrogenation and subsequent rehydrogenation at C5,15.¹³ Since there is no hydrogen acceptor present in solution, and hydrogenation of porphyrins at the bridge positions requires rather strong reducing agents, e.g. metallic zinc in acetic acid, it seems more likely that a transitory ring opening occurs at C5,15. As the nickel insertion is run in acetic acid, it competes with the isomerization. Once the nickel chelate is formed, ring opening is no longer possible, and a certain fraction of the original anti isomer is thus saved by coordination.

Once isolated, *ae-3* is stable indefinitely in the solid state and in nonprotic solvents such as toluene and chloroform. Its UV/vis and IR spectra are distinctly different from the spectra of its isomer, *aa-3* (see Experimental Section), especially the longest wavelength optical absorption, which appears bathochromically shifted by about 18 nm. Such a bathochromic shift could indicate a somewhat greater distortion of the pyrromethene chromophore of *ae-3* from planarity as compared with that of *aa-3*.¹⁴ In the IR spectrum, the porphodimethene band appearing between 873

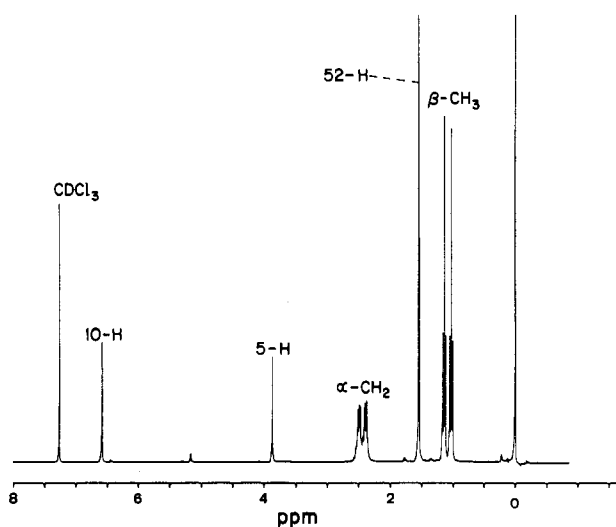


Figure 1. ¹H NMR spectrum of Ni(OEPBu₂) (*aa-4*) in CDCl₃ at 20 °C.

and 901 cm⁻¹ in the syn-axial Ni^{II} complexes is shifted to 960 cm⁻¹ for *ae-3*. The mass spectra are the same apart from some variation of the intensities of the peaks.

The ¹H NMR spectra of these nickel(II) porphodimethenes show many expected similarities but also some interesting differences related to structural changes occurring within the series. The assignments, chemical shifts, and coupling constants are listed in Table I along with data for nickel(II) octaethylporphyrin for comparison. A representative spectrum, that of Ni(OEPBu₂), *aa-4*, is shown in Figure 1 and is consistent with the syn-axial, C_{2v} geometry. All syn-axial complexes exhibit one set each of H5,15, H10,20, H51, and H52 resonances and two sets of α-CH₂ and β-CH₃ resonances.

An important feature for the assignment of the spectra was the observation that the geminal α-CH₂ protons of each of the two sets of the peripheral ethyl groups are diastereotopic. This phenomenon results from the inherent axial asymmetry of the porphodimethene macrocycle. An analogous situation previously was documented for the axially asymmetric thallium(III) or lead(II) octaethylporphyrins, such as (H₂O)Tl(OEP)(OH) or Pb(OEP), for which the ¹H NMR spectrum shows a set of overlapping, anisochronous α-CH₂ resonances.^{15,16} Further recent examples are the metal-metal-bonded bis(porphyrins) Rh₂(OEP)₂¹⁷ and Mo₂(OEP)₂¹⁸ as well as the cerium(IV) sandwiched Ce(OEP)₂.¹⁹ In all these systems, the asymmetry is due to the fact that the spaces above and below the porphyrin plane are not

(12) We have no evidence for the formation of *anti*-Ni(OEPR₂) as the dd stereoisomer. This could be very easily identified from its ¹H NMR spectrum.

(13) Paine, J. B., III. In *The Porphyrins*; Dolphin, D., Ed.; Academic: New York, 1978; Vol. I, p 166.

(14) Brunings, K. J.; Corwin, A. H. *J. Am. Chem. Soc.* **1942**, *64*, 593.

(15) Abraham, R. J.; Barnett, G. H.; Smith, K. M. *J. Chem. Soc., Perkin Trans. 1* **1973**, 2142.

(16) Busby, C. A.; Dolphin, D. *J. Magn. Reson.* **1976**, *23*, 211.

(17) Ogoishi, H.; Setsune, J.; Yoshida, Z. *J. Am. Chem. Soc.* **1977**, *99*, 3869.

(18) Collman, J. P.; Barnes, C. E.; Woo, L. K. *Proc. Natl. Acad. Sci. U.S.A.* **1983**, *80*, 7684.

(19) Buchler, J. W.; De Cian, A.; Fischer, J.; Kihn-Botulinski, M.; Paulus, H.; Weiss, R. *J. Am. Chem. Soc.* **1986**, *108*, 3652.

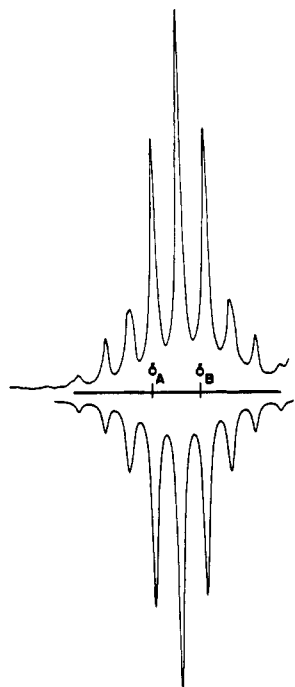


Figure 2. Comparison of the observed (top) and simulated (bottom) ABX_3 multiplet (1H NMR, 300 MHz) for α - CH_2 protons in Ni(OEP-Me₂) (*aa-1*).

identical, whereas with the porphodimethene the axial asymmetry is inherent in the macrocycle.

For the α - CH_2 protons of *aa-1*–*aa-3* a simple A_2X_3 quartet and a complex ABX_3 multiplet are observed. It is assumed that the simpler A_2X_3 pattern, where the diastereotopism of the geminal pair is not evident, is due to the α - CH_2 protons adjacent to C10,20. For *aa-4*, two ABX_3 multiplets are observed. In all four complexes the pyrrole methyl proton resonances appear as two sets of triplets with $J_{AX} = J_{BX} = 7.6$ Hz. Selective decoupling of these β - CH_3 resonances allows for unequivocal assignment of which α - CH_2 and β - CH_3 signals are coupled together. For example, irradiation of the high-field β - CH_3 triplet at 1.02 ppm in *aa-4* causes collapse of the α - CH_2 multiplet at 2.38 ppm to an AB pattern. Coupling constants and chemical shifts for the α - CH_2 protons (ABX_3) were determined precisely by computer simulation of the multiplet. The result for *aa-1*, which is typical, is as follows: $\delta_A = 2.50$, $\delta_B = 2.45$, $J_{AB} = 14.1$ Hz, RMS = 8.0×10^{-4} ppm. The simulated spectra are in good agreement with the observed spectra, as can be seen in Figure 2 for the α - CH_2 multiplet in *aa-1* centered at 2.48 ppm. The geminal proton coupling constant of 14 Hz is consistent with that observed in other systems, as for example in derivatives of (diethylglyoximate)nickel(II).²⁰

The configuration of the anti isomer of Ni(OEPPr₂), *ae-3*, is confirmed by an analysis of its 1H NMR spectrum. This molecule has a mirror plane along C5,15 as the only symmetry element. Therefore, the following NMR spectrum is expected: two sets of signals for the H5,15, H51, and H52 protons respectively, and four sets of signals for the α - CH_2 and β - CH_3 protons, respectively, but only one signal for H10,20. This pattern is indeed observed (see Table I). The assignments of the axial and equatorial resonances can be made by comparison with the spectrum for *aa-3*, the syn-axial isomer. For example, the H5,15 resonances of *ae-3* are both doublets at 3.36 and 5.43 ppm. The former is assigned as equatorial because of its correspondence to the 3.56 ppm resonance in *aa-3*, whereas the 5.43 ppm resonance is axial with no corresponding signal to be found in *aa-3*. A complete assignment is listed in Table I.

For each set of H5,15, H51, and H52 protons, there is a pair of axial and equatorial resonances. In all three cases the equatorial protons are more shielded, and the chemical shift difference, δ_{ax}

– δ_{eq} , for two of the sets is large: 2.1 ppm for the H5,15 pair and 1.4 ppm for the H51 pair. In comparison, a difference of only 0.4–0.8 ppm is encountered for the axial and equatorial protons in monosubstituted cyclohexanes.²¹ This large difference in *ae-3* must be related to the neighboring magnetic environment rather than internal inductive effects. The equatorial H5,15 and H51 protons sit in a pocket closely surrounded by the peripheral ethyl groups of the adjacent pyrroles. This should result in significant long-range shielding of the equatorial protons compared to that for the axial protons.

The vicinal coupling constant for the axial H5,15 proton in *ae-3* is unusually high, 12.8 Hz, and is strong evidence for steric crowding and lack of free rotation for the attached equatorial isopropyl group. According to the Karplus relationship, this value is consistent with a dihedral angle of 0 or 180° between the two vicinal CH bond vectors. An angle of 180° seems preferable since the two methyls of the equatorial isopropyl group would then be more distant from the adjacent ethyl groups of the pyrrole rings. If the isopropyl group is freely rotating, an averaged vicinal coupling constant of 5–8 Hz is expected.²² It is impossible to know whether any unusual degree of folding or ruffling of the porphodimethene occurs because of this steric crowding.

Some patterns appear in the chemical shifts for the nickel(II) porphodimethenes. For the syn-axial series, there is a systematic increase in chemical shift of the axial protons, H51 or H52, as the size of R increases. This pattern is commonly observed for alkyl substituents and has been previously documented.²³

The H5,15 chemical shifts in the syn-axial series vary in an irregular fashion, first decreasing from 3.97 to 3.56 ppm from *aa-1* to *aa-3* and then increasing to 3.87 ppm in *aa-4* when R = *tert*-butyl. This is probably related to structural changes within the series. For example, the degree of steric interaction between axial alkyl groups, the extent of folding, and the extent of ruffling are all variables that change with increasing size of R. All will affect the chemical shift of H5,15; however, without detailed structural data for the four syn-axial complexes, a precise explanation is impossible.

The most noticeable feature in the NMR spectra of all five nickel(II) porphodimethenes reported herein is the increased shielding for all protons as compared to that for the analogous protons in Ni(OEP) (Table I). This clearly is a consequence of the reduced aromaticity and is especially pronounced for the H10,20 proton resonances, which have shifted 3 ppm upfield as compared to those of Ni(OEP). These protons, sitting at the methene bridges between the pyrrole rings of each of the pyrromethene halves, may be used as planarity probes of the pyrromethene parts and hence may indicate a saddlelike deformation of the systems. In a planar pyrromethene, H10,20 should experience the largest downfield shift due to a ring current effect of the adjacent two pyrrole units. If H10,20, for example, is forced to leave the planes of these neighboring pyrrole rings due to a ruffling of the pyrroles, a slight upfield shift should be observed. The chemical shifts of H10,20 decrease in the order *aa-1* \approx *aa-2* > *aa-3* > *aa-4* > *ae-3* (see Table I) and indicate that the porphodimethenes with the smallest 5,15-substituents have the smallest saddlelike deformation. Following this argument, the unusual *ae-3* seems to have the largest deformation in this respect, demonstrating the awkward geometry of the anti isomer.

Acknowledgment. This work was supported by the Deutsche Forschungsgemeinschaft, the Fonds der Chemischen Industrie (Frankfurt, West Germany), the Vereinigung von Freunden der Technischen Hochschule Darmstadt, and a collaborative research grant from NATO. Thanks are due to Dr. S. Braun for help with the Bruker NMR spectrometer and Priv.-Doz. Dr. M. Veith for mass spectra.

(21) Jackman, L. M.; Sternhell, S. *Applications of Nuclear Magnetic Resonance in Organic Chemistry*, 2nd ed.; Pergamon: Oxford, England, 1969; pp 78–80.

(22) See ref 20, pp 280–283.

(23) Becker, E. *High Resolution NMR*, 2nd ed.; Academic: New York, 1980; pp 72–73.